Effects of Age on Peripapillary and Macular Vessel Density Determined Using Optical Coherence Tomography Angiography in Healthy Eyes

Youn Hye Jo, Kyung Rim Sung, and Joong Won Shin

Department of Ophthalmology, University of Ulsan, College of Medicine, Asan Medical Center, Seoul, Korea

Correspondence: Kyung Rim Sung, Department of Ophthalmology, University of Ulsan, College of Medicine, Asan Medical Center, 88, Olympic-Ro 43-Gil, Songpa-Gu, Seoul 05505, Korea;
sungeye@gmail.com.

Submitted: February 8, 2019
Accepted: July 10, 2019

Citation: Jo YH, Sung KR, Shin JW. Effects of age on peripapillary and macular vessel density determined using optical coherence tomography angiography in healthy eyes. *Invest Ophthalmol Vis Sci*. 2019;60:3492–3498. https://doi.org/10.1167/iovs.19-26848

Purpose. To evaluate the effect of age on global and sectoral vascular parameters of the peripapillary area and macula in healthy eyes by using optical coherence tomography angiography (OCT-A).

Methods. This retrospective cross-sectional study included 239 eyes of 172 healthy subjects. Subjects were scanned using the high-definition disc angio scan (4.5 × 4.5 mm), retina angio scan (6 × 6 mm), and optic nerve head/ganglion cell complex (GCC) modes of OCT-A. Global and sectoral circumpapillary vessel density (VD), parafoveal VD, retinal nerve fiber layer (RNFL), and GCC thickness parameters were modeled in terms of age by using linear mixed-effect models incorporating covariates. Normalized slopes were calculated by dividing the absolute slopes by the mean value of the OCT-A parameters.

Results. All global and sectoral circumpapillary VDs decreased significantly with increasing age, except for those in the temporal superior sector. The steepest slopes in the circumpapillary region were observed in nasal superior (−0.098%/y) and nasal inferior (−0.096%/y) sectors. The global, temporal, and superior macular VDs also decreased with increasing age, while the foveal, nasal, and inferior parameters did not. The temporal quadrant showed the steepest slope among the macular parameters (−0.068%/y). The RNFL and GCC thickness results showed similar trends.

Conclusions. Age substantially affected VD in most of the peripapillary and macular areas; however, the papillomacular bundle area did not show significant age-related vascular changes. These age-related global and sectoral differences in circumpapillary and macular VDs should be considered when assessing pathologic VD changes over time.

Keywords: vessel density, optical coherence tomography angiography, optic nerve head, macula

Optical coherence tomography angiography (OCT-A) is a newly developed technique that allows noninvasive evaluation of retinal vasculature.[1] OCT-A has shown good reproducibility in measuring the ocular vascular structure quantitatively and has potential for use as an adjunctive diagnostic tool for glaucomatous damage.[2,3] Quantitative assessment of ocular vascular structures is potentially valuable in clinical practice because it allows the comparison of structures over time. In many previous studies, glaucomatous eyes have shown reduced vascular density than do healthy eyes.[3–5] However, to detect changes in OCT-A measurements associated with glaucomatous damage, normal physiologic aging effects on the vasculature should be considered. Needless to say, changes beyond the physiologic level can be explained by pathologic alterations. However, it is oftentimes difficult to differentiate between these pathologic alterations and physiologic age-related changes.

Previous studies have reported the age-related changes in the retinal vasculature and choriocapillaris measured using OCT-A in healthy subjects[6,7]; however, these studies focused on the macular vasculature. Although the valuable role of the circumpapillary parameters of OCT-A in glaucoma practice has been highlighted in several studies,[4,8,9] research regarding age-related changes in the peripapillary region is scarce.[6,10] In particular, the rates of age-related change in the global and sectoral regions of circumpapillary and macular vessel densities have not been previously published.

The purpose of the current study was to evaluate the age-related changes in peripapillary and macular parameters measured using OCT-A in healthy eyes. We assessed the global and regional rates of change to test the hypothesis that aging would affect the peripapillary and macular retinal vasculature. Further, we aimed to investigate whether the rate of change differed among different sectors in the posterior segment because glaucoma begins as a localized change. To the best of our knowledge, this is the first study to evaluate the age-related changes in vessel density (VD) in the global and regional peripapillary and macular areas of healthy subjects.

Methods

Subjects

This was a retrospective, cross-sectional study performed on healthy subjects who visited the ophthalmology outpatient clinic of Asan Medical Center, Seoul, Korea. The subjects were

either who attended the clinic with mild ocular problem, such as dry eye syndrome or blepharoconjunctivitis or those who wanted to do routine check-up in their eyes. The study was approved by the institutional review board Ethics Committee of Asan Medical Center and adhered to the tenets of the Declaration of Helsinki.

All subjects underwent a comprehensive ophthalmologic examination, which included a detailed medical history for conditions, such as hypertension (HTN) and diabetes mellitus (DM), best-corrected visual acuity (BCVA) measurement with refractive error, slit-lamp biomicroscopy, IOP measurement with Goldmann applanation tonometry, axial length measurement with IOL master (Cal Zeiss Meditec, Dublin, CA, USA), gonioscopy, dilated color fundus and stereoscopic photography of the optic nerve head (ONH), and red-free retinal nerve fiber layer (RNFL) photography (Canon, Tokyo, Japan). The subjects also completed Humphrey perimetry using the Swedish Interactive Threshold Algorithm 24-2 (Carl Zeiss Meditec).

The inclusion criteria were as follows: age 18-years old or older, BCVA over 20/40, spherical equivalent within 6.0 diopters (D), no medial opacities that affect fundus imaging, normal clinical ocular examination findings with no evidence of retinal or ONH pathologies, IOP 21 mm Hg or less, open angles on gonioscopy, and normal 24-2 visual field (VF) results. A normal VF was defined as a glaucoma hemifield test result within normal limits and pattern standard deviation probability greater than 5%. Eyes suspected of having glaucoma, cup-to-disc (C/D) ratio greater than 0.7, asymmetry of the C/D ratio greater than 0.2, neuroretinal rim thinning, notching, or RNFL defects were excluded. Eyes were also excluded if they had a history of inflammation, trauma, and any previous intraocular surgery except for uncomplicated cataract extraction. If both the eyes were eligible, both were included in this study.

Optical Coherence Tomography Angiography

All OCT-A scans of the ONH and macula were performed using RTVue-XR (software version 2017.01, Angiovue; Optovue Inc., Fremont, CA, USA) in the high-definition (HD) disc scan (4.5 × 4.5 mm), HD retina scan (6 × 6 mm), and ONH/ganglion cell complex (GCC) scan modes. Details of the OCT-A measurements have been described elsewhere.[4,11–13] The whole en face image of the disc and macular area were scanned, and the software automatically measured VD defined as the percentage of the area occupied by the large vessels and microvasculature in a certain region. In circumpapillary region, we used the data obtained by built-in program, which offers the data excluding the large vessels automatically. Circumpapillary VD (cpVD) was calculated in the radial peripapillary capillary (RPC) layer, which is a unique vascular plexus in the RNFL, of the 1-mm wide elliptical annulus extending from the optic disc boundary. The circumpapillary region was divided into eight sectors on the basis of the modified Garway-Heath map[14] and cpVD within each sector was assessed. Macular VD was analyzed over a 1-mm wide parafoveal circular annulus centered on the fovea. Parafoveal VD (pfVD) analyzed in this study included the superficial vascular plexus extending from the internal limiting membrane (ILM) to the inner plexiform layer (IPL). This area was also divided into four quadrants at 90°, namely, the superior, inferior, nasal, and temporal sectors. In addition, the RNFL thickness at 3.45-mm diameter was measured relative to the disc center for each eight sectors on ONH map and the GCC thickness was measured from ILM to IPL in the superior hemiretina, inferior hemiretina, and overall.

All images acquired using OCT-A were assessed for their image quality. The eyes with signal strength index (SSI) over 45, motion artifacts, or projection artifacts caused by floaters were excluded. The SSI value of each scan (HD disc, macular, and ONH/GCC scan) was used for analysis as a covariate.

Statistical Analysis

The parameters used for analyzing the peripapillary measurements were eight-sectoral VDs and RNFL thicknesses, and those for analyzing the macular measurements were four-sectoral VDs, and two hemiretina GCC thicknesses obtained automatically.

Linear mixed-effect models were used to assess the changes in OCT-A parameters across subjects having different ages. All the determinant variables,[6,10,15–17] which are known to affect VD—age, sex, axial length, central corneal thickness, IOP, SSI, and history of DM and HTN—were treated as fixed-effect parameters, and the subject was treated as a random-effect parameter. The absolute slope for the sectoral parameter measurements over different age groups was calculated. To evaluate whether the relative rate of change was similar throughout the different sectors, we normalized the slope values by calculating the slope divided by the average parameter value, because the rate of change might be affected by the extent of the measurement.

All statistical analyses were performed using R program version 3.5.1 (R Foundation for Statistical Computing, Vienna, Austria) and PASW Statistics for Windows/Macintosh, Version 18.0 (SPSS Inc., Chicago, IL, USA). $P < 0.05$ was considered statistically significant.

Results

In total, 239 eyes of 172 healthy subjects were enrolled in this study. Nine of these eyes were excluded from the macular analysis because of projection artifacts caused by floaters in the macula. Of the 172 subjects, 106 were women and 66 were men, and all were Asian (Korean). The mean (±SD) age was 52.5 ± 14.3 years, and the ages ranged from 18 to 83 years. The distribution of ages is presented in Figure 1. Table 1 shows the demographic parameters of the included subjects in the different age groups. The mean cpVD was 52.48 ± 2.32%, and the mean pfVD was 52.54 ± 3.63%. The mean RNFL thickness was 103.33 ± 6.66 and the mean GCC thickness was 97.38 ± 4.94. The number of eyes included for each scan type and the measurements of global and sectoral cpVD, RNFL thickness, pfVD, and GCC thickness parameters across the different age groups are summarized in Tables 2 and 3.

The slope of cpVD over different age was statistically significantly different from the slope of zero for global and in the following seven sectors: superotemporal (ST), superonasal (SN), temporal inferior (TI), inferotemporal (IT), inferonasal (IN), nasal superior (NS), and nasal inferior (NI) ($P < 0.05$), but the temporal superior (TS) sector showed no statistically significant change ($P = 0.456$). The NS (–0.098%/y, normalized, –0.002; $P < 0.001$) and NI sectors (–0.096%, normalized, –0.002; $P < 0.001$, Table 4) had the steep slopes.

The slope of RNFL thickness over different age also showed similar result with that of cpVD. The slope of RNFL thickness for global and seven sectors, ST, SN, TI, IT, IN, NS, and NI, was significantly different from the slope of zero ($P < 0.05$), while TS sector did not ($P = 0.063$; Table 4).

The pfVD statistically significantly decreased by –0.051%/y (normalized, –0.00097; $P = 0.008$) according to increasing age, but no statistically significant change was observed in the fovea at –0.018%/y (normalized: –0.00088; $P = 0.695$). The temporal sector showed the steep slope at –0.068%/y (normalized: –0.0013; $P = 0.002$), but the nasal and inferior sectors showed no significant change (Table 5).

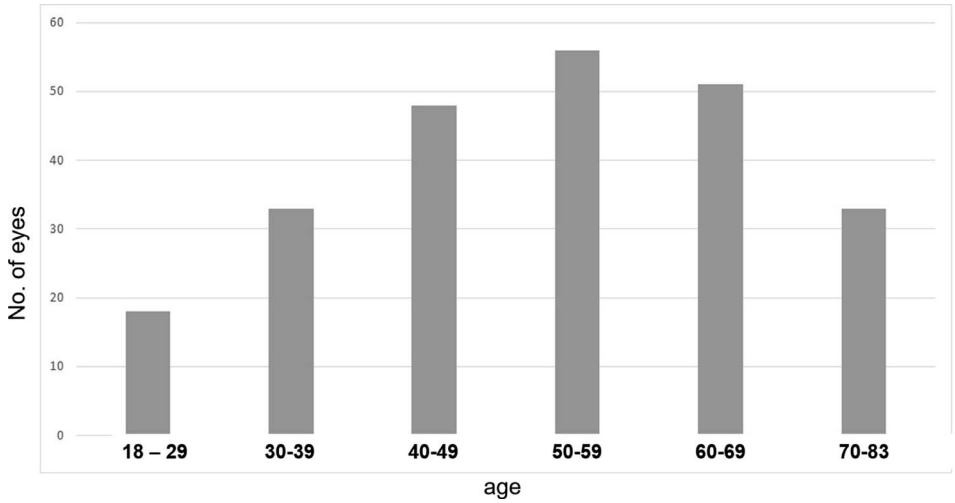

Figure 1. Age distribution of the study subjects by decade.

The average GCC thickness also decreased by –0.063%/y with marginal significance (normalized, –0.00065; $P = 0.057$) and superior hemiretina GCC thickness showed significant decrease by –0.072%/y (normalized, –0.00074; $P = 0.031$; Table 5). In the meantime, inferior hemiretina (–0.061%/y normalized, –0.00062; $P = 0.094$) did not show statistically significant decrease. Scatter plots with fit lines of average cpVD, RNFL thickness, and GCC thickness against age were illustrated in Figure 2.

Discussion

In previous studies, RNFL and macular thicknesses showed global and regional reductions with age.[18–21] On the basis of these results, we expected that the RPC supplying the RNFL layer and the superficial retinal VD distributed in the inner retina would subsequently decrease. Otherwise, the reduction of VD could be a primary event associated with aging; however, this issue was not explored in this study. Our study demonstrated that VD significantly decreased in most of the peripapillary and macular regions as the participants' age increased.

In previous studies, RNFL and macular thicknesses showed different rates of change in different sectors according to aging.[18] As with the structural aging effect, the microvasculature would also change at different speeds in different regions. In terms of peripapillary RNFL thickness, the temporal quadrant and region corresponding to clock-hour 10 showed no significant differences with aging in that study. Leung et al.[22] also revealed that the temporal side of the optic disc showed no significant change over time in their longitudinal study. Our results of RNFL thickness were in the same line with these previous studies. Similarly, we found that the slope of cpVD in the TS sector did not significantly differ from the slope of zero. Further, the TI and IT sectors of cpVD showed the relatively flat slopes with marginal significance ($P = 0.040$ and $P = 0.042$, respectively). Hence, like RNFL thickness, cpVD showed no dramatic decline of VD on the circumpapillary temporal sectors. This result coincided with that obtained for macular VD. The nasal side of the macula, which is the temporal side of the optic disc, did not show a significant difference with aging in terms of VD. Therefore, VD in the papillomacular bundle area seems relatively well-preserved during aging in our current study.

Interestingly, cpVD of the nasal quadrant showed the steep slope (NS and NI; normalized slope, –0.002 and –0.002, respectively; $P < 0.001$); however, this feature was not noticeable in RNFL thickness analysis. RNFL thickness showed relatively similar level of slope in all sectors except for TS sector. This may be due to the proportion of nonneuronal tissue, such as glial tissue, within the RNFL, which has been reported to increase with age.[23,24] RNFL thickness determined by OCT includes both neuronal layer, such as RNFL and nonneuronal tissue.[23–25] Axonal fibers in the RNFL decrease with age, indicating an inverse relationship between its thickness and the proportion of nonneuronal tissue. Thus, the RNFL may change less according to age, as measured by OCT, owing to offsets caused by a combination of the decreased width of neuronal tissue and increased width of nonneuronal tissue. In the meantime, as neuronal tissue itself decreases with aging, cpVD may undergo more reduction. However, various studies showed different patterns of RNFL

Table 1. Clinical Demographics of the Participants

Age, y	18–29	30–39	40–49	50–59	60–69	70–85	Total
N of eyes	18	33	48	56	51	33	239
Mean Age	25.11 ± 4.26	35.88 ± 2.32	45.77 ± 3.03	53.98 ± 2.82	63.78 ± 3.05	73.94 ± 3.62	52.51 ± 14.32
Sex (M:F)	9:9	25:8	32:16	31:25	31:20	20:13	148:91
Axial length, mm	25.41 ± 0.78	24.55 ± 1.11	24.27 ± 0.87	23.77 ± 0.93	23.67 ± 0.69	23.79 ± 0.94	24.12 ± 1.02
IOP, mm Hg	14.0 ± 2.85	13.64 ± 2.73	14.67 ± 3.01	14.13 ± 2.50	14.12 ± 2.73	13.79 ± 2.83	14.11 ± 2.75
CCT, μm	532.58 ± 37.14	532.50 ± 39.56	558.29 ± 38.62	540.98 ± 33.19	537.69 ± 35.08	528.19 ± 28.05	540.33 ± 36.71
DM, n (%)	0 (0)	0 (0)	3 (6.3)	3 (5.4)	4 (7.8)	6 (18.2)	16 (6.7)
HTN, n (%)	0 (0)	0 (0)	8 (16.7)	11 (19.6)	18 (35.3)	12 (36.4)	49 (20.5)

Data are represented by mean standard deviation values.

Table 2. Circumpapillary Vessel Densities and Retinal Nerve Fiber Layer Thickness for Global and Eight Sectors in Different Age Groups

Age, y	18–29	30–39	40–49	50–59	60–69	70–85	Total
N of eyes	18	33	48	55	51	34	239
cpVD							
SSI	72.22 ± 6.96	75.52 ± 8.11	75.02 ± 7.67	73.95 ± 8.36	73.71 ± 8.43	65.50 ± 7.62	73.06 ± 8.52
Average	52.87 ± 2.10	53.84 ± 2.21	53.48 ± 1.78	51.62 ± 2.19	52.13 ± 2.24	50.99 ± 2.24	52.42 ± 2.32
ST	56.10 ± 3.19	56.65 ± 3.46	56.46 ± 2.63	54.53 ± 3.43	55.19 ± 3.21	54.28 ± 3.53	55.44 ± 3.33
SN	51.55 ± 3.48	52.49 ± 3.67	51.85 ± 3.13	49.42 ± 3.58	50.86 ± 3.68	49.73 ± 4.23	50.85 ± 3.75
TS	56.06 ± 3.02	56.65 ± 3.46	58.19 ± 2.87	56.39 ± 3.09	56.60 ± 3.73	55.84 ± 3.73	56.90 ± 3.10
TI	53.71 ± 3.79	56.02 ± 3.31	55.57 ± 3.44	53.77 ± 3.50	53.52 ± 3.20	52.29 ± 3.60	54.18 ± 3.61
IT	56.41 ± 3.02	58.47 ± 3.78	57.74 ± 3.66	56.57 ± 3.92	55.96 ± 4.00	53.22 ± 3.19	57.02 ± 3.78
IN	51.26 ± 3.76	52.95 ± 3.98	52.02 ± 3.66	50.34 ± 3.91	51.16 ± 4.44	50.32 ± 4 .27	51.28 ± 4.09
NS	50.31 ± 3.36	50.06 ± 3.15	50.21 ± 2.74	48.25 ± 3.21	48.67 ± 3.16	46.20 ± 3.42	48.87 ± 3.38
NI	49.84 ± 2.66	49.32 ± 3.56	49.08 ± 3.09	46.69 ± 4.37	47.42 ± 3.18	46.53 ± 3.87	47.91 ± 3.76
RNFL thickness							
SSI	70.50 ± 7.96	70.55 ± 7.78	71.33 ± 7.54	70.69 ± 6.98	69.61 ± 8.55	63.82 ± 8.01	69.60 ± 8.06
Average	103.44 ± 108.03	108.03 ± 6.72	103.90 ± 4.61	102.71 ± 6.89	102.35 ± 6.24	100.27 ± 7.33	103.33 ± 6.66
ST	141.61 ± 11.06	145.85 ± 12.23	142.92 ± 10.54	138.62 ± 12.07	138.39 ± 11.48	136.30 ± 13.83	140.34 ± 12.14
SN	114.56 ± 9.97	122.82 ± 14.53	114.44 ± 13.52	112.35 ± 15.50	113.69 ± 13.54	110.45 ± 11.76	114.41 ± 14.04
TS	88.44 ± 14.04	91.03 ± 10.47	89.46 ± 10.18	87.33 ± 10.22	83.96 ± 7.94	86.06 ± 11.01	87.46 ± 10.24
TI	70.72 ± 8.64	76.30 ± 9.93	74.83 ± 8.11	75.55 ± 7.52	71.71 ± 6.75	71.12 ± 10.01	73.01 ± 8.44
IT	144.83 ± 16.21	151.42 ± 14.53	147.17 ± 11.69	146.11 ± 11.94	143.47 ± 11.49	139.85 ± 17.18	145.53 ± 13.62
IN	116.22 ± 13.99	119.21 ± 12.49	110.48 ± 11.40	112.56 ± 13.76	113.73 ± 14.08	109.85 ± 13.51	113.21 ± 13.39
NS	79.33 ± 8.22	82.30 ± 10.14	78.79 ± 8.03	78.87 ± 9.38	79.90 ± 8.73	77.67 ± 8.87	79.42 ± 8.95
NI	72.39 ± 7.33	77.09 ± 10.57	72.85 ± 6.49	72.76 ± 6.50	72.08 ± 6.93	70.36 ± 7.84	72.87 ± 7.67

Data are mean ± standard deviation values.

change in nasal and temporal sectors according to aging.[18,21,26–28] For instance, a recent study by Wang et al.[29] investigated over 5000 subjects of ages between 20 and 80 and reported the largest age effect in the temporal and the smallest age effect in the nasal sector. Different study population, design, and methodology may contribute to substantial variation of the age-related decline in RNFL thickness over different studies.

Differences in the rate of decrease were also found within the macular region. VD of the fovea, which is devoid of superficial layer vasculature, remains stable throughout life. Because there is no RNFL in the fovea, superficial layer VD may be too scarce to be detected by OCT-A in that layer, which may lead to minimal change with aging. These results showing different rates in different areas were in line with the known distribution of the nerve fiber bundles in the eye. The concentration of thinner nerve fibers on the temporal side of the ONH and nasal side of the macula has been reported in a previous histologic study.[30] Despite the same extent of axonal loss, the region with the greater concentration of thinner nerve fibers will show a shallower reduction. This would show similar results in the vascular structures supplying blood to those regions. Another possible explanation is that vascular reduction in the retina will be maintained in the direction of preservation of vision, which will be reflected in the slower rates of change in the papillomacular bundle region.

A few recent studies have reported the determinants of VD measured using OCT-A. However, these studies were generally restricted to the macular region or evaluated the effects on VD.[6,10,31,32] Yu et al.[10] evaluated the effect of age and sex on

Table 3. Parafoveal Vessel Densities for Global and Four Quadrants and Ganglion Cell Complex Thickness for Global, Superior, and Inferior Hemiretina in Different Age Groups

Age, y	18–29	30–39	40–49	50–59	60–69	70–79	Total
N of eyes	18	33	48	55	47	29	230
pfVD							
SSI	68.94 ± 5.34	71.58 ± 6.75	72.54 ± 5.69	69.60 ± 6.50	69.57 ± 6.14	64.10 ± 4.79	69.75 ± 6.46
Foveal VD	25.60 ± 6.54	19.80 ± 7.40	19.71 ± 7.39	19.57 ± 6.06	20.17 ± 7.48	19.84 ± 8.45	20.26 ± 7.29
Average	52.79 ± 2.60	53.63 ± 3.31	54.35 ± 2.79	52.41 ± 2.93	51.83 ± 3.70	49.07 ± 4.29	52.48 ± 3.63
Sup. hemi	53.45 ± 3.05	54.02 ± 3.01	54.91 ± 2.83	52.53 ± 2.84	52.27 ± 3.88	49.28 ± 4.55	52.85 ± 3.73
Inf. hemi	52.33 ± 2.63	53.23 ± 3.95	54.02 ± 2.94	52.29 ± 3.48	51.44 ± 3.89	49.21 ± 4.11	52.23 ± 3.81
T	52.84 ± 3.20	53.27 ± 3.35	53.91 ± 3.33	52.40 ± 3.58	51.91 ± 3.48	48.54 ± 4.52	52.29 ± 3.88
S	54.23 ± 3.27	54.69 ± 3.67	55.28 ± 3.57	52.83 ± 3.29	52.21 ± 4.63	49.84 ± 4.98	53.21 ± 4.26
N	52.17 ± 3.19	52.80 ± 3.47	53.87 ± 3.19	51.69 ± 3.55	51.87 ± 3.88	48.59 ± 4.45	51.98 ± 3.91
I	51.94 ± 3.27	53.75 ± 4.46	54.35 ± 3.25	52.73 ± 3.69	51.56 ± 4.44	49.40 ± 4.96	52.49 ± 4.21
GCC thickness							
SSI	70.13 ± 7.72	77.00 ± 7.39	75.67 ± 6.97	75.02 ± 6.38	73.05 ± 9.59	68.67 ± 5.49	73.80 ± 7.78
Average	97.00 ± 5.25	98.28 ± 4.65	97.58 ± 4.34	98.86 ± 4.82	95.98 ± 4.96	95.87 ± 5.76	97.38 ± 4.94
Sup. hemi	97.75 ± 4.81	98.71 ± 4.88	97.67 ± 4.46	98.49 ± 4.96	95.49 ± 4.31	95.90 ± 5.65	97.34 ± 4.93
Inf. hemi	96.38 ± 5.81	98.16 ± 5.24	97.58 ± 5.02	99.10 ± 5.19	96.16 ± 5.10	96.07 ± 6.24	97.44 ± 5.42

Sup., superior; Inf, inferior; hemi., hemiretina. Data are mean ± standard deviation values.

Table 4. Absolute and Normalized Slopes of cpVD and RNFLT in Terms of Age as Determined Using OCT-A (With Confidence Intervals and *P* Values for Absolute Slopes)

	Intercept	Absolute Slope	Confidence Interval	*P* value	R^2	Normalized Slope
cpVD						
Average	66.22	−0.065	−0.093 to −0.037	<0.001*	0.735	−0.00124
Sup. hemi	65.71	−0.059	−0.088 to −0.030	<0.001*	0.730	−0.00111
Inf. hemi	66.48	−0.071	−0.103 to −0.040	<0.001*	0.701	−0.00137
ST	70.79	−0.054	−0.095 to −0.014	0.008*	0.723	−0.00098
SN	58.14	−0.046	−0.092 to 0.000	0.047*	0.636	−0.00090
TS	54.05	−0.015	−0.054 to 0.024	0.456	0.542	−0.00026
TI	50.01	−0.047	−0.092 to −0.002	0.040*	0.624	−0.00087
IT	77.45	−0.047	−0.094 to −0.001	0.042*	0.731	−0.00083
IN	78.22	−0.082	−0.130 to −0.034	0.001*	0.644	−0.00159
NS	71.69	−0.098	−0.139 to −0.058	<0.001*	0.573	−0.00201
NI	60.45	−0.096	−0.140 to −0.051	<0.001*	0.544	−0.00200
RNFLT						
Average	132.70	−0.185	−0.265 to −0.104	<0.001*	0.958	−0.00179
Sup. hemi	138.43	−0.185	−0.277 to −0.093	<0.001*	0.950	−0.00175
Inf. hemi	137.06	−0.196	−0.281 to −0.110	<0.001*	0.913	−0.00193
ST	164.56	−0.222	−0.373 to −0.071	0.004*	0.816	−0.00158
SN	158.65	−0.246	−0.419 to −0.073	0.005*	0.868	−0.00215
TS	79.05	−0.116	−0.239 to 0.008	0.063	0.674	−0.00133
TI	80.96	−0.112	−0.213 to −0.011	0.028*	0.851	−0.00154
IT	194.12	−0.307	−0.472 to −0141	<0.001*	0.804	−0.00211
IN	200.35	−0.283	−0.446 to −0.117	0.001*	0.840	−0.00250
NS	134.18	−0.168	−0.272 to −0.064	0.001*	0.537	−0.00212
NI	94.44	−0.146	−0.241 to −0.050	0.003*	0.801	−0.00200

* *P* value for an absolute slope different from a zero slope.

macular VD and reported that pfVD decreased with increasing age (0.4%/y). We also found a decrease in cpVD (–0.061%/y) as well as pfVD (–0.116%/y). In contrast, Gadde et al.[32] and Rao et al.[6] reported that although pfVD decreased with age (0.2%/y), the decrease did not reach statistical significance. In the study by Rao et al.,[6] cpVD was also unaffected by age. The reason for these discrepancies might be the methods used for measuring VD. The software we used for estimating VD was different from those used in previous studies. We used the VD values provided automatically by the software (version 2017.01), which fit an ellipse to the optic disc margin and defined the peripapillary region as a 1-mm wide elliptical annulus. It also automatically differentiated between capillaries and large vessels in peripapillary area; therefore, we could use the data of capillaries for analysis. However, Rao et al.[6] used a software (version 2015.100.0.33) that defined the peripapillary region as a 0.75-mm wide elliptical annulus, and thus could not differentiate between capillaries and large vessels. The earlier studies used either a set threshold decorrelation value obtained using ImageJ[10] or local fractal analysis[32] to calculate VD. The mean pfVD in our study was 52.54%, whereas it was 26.6% in the study by Wang et al.[31], and 89.1% in the study by Yu et al.[10] The mean superficial pfVD determined using local fractal analysis[32] (50%) and the embedded software[6] (50.4%) was similar to that determined in the present study. Therefore, the method of VD evaluation should be considered when analyzing the difference in VD reported in all of these studies.

Our study has some limitations that should be considered. First, our study was cross-sectional. If we could follow the change in VD in each individual longitudinally, it would be ideal. However, this was not practical in the present stage using new technology. Therefore, we acknowledge that we are not

Table 5. Absolute and Normalized Slopes of Parafoveal VD in Terms of Age as Determined Using OCT-A (With Confidence Intervals and *P* Values for Absolute Slopes)

	Intercept	Absolute Slope	Confidence Interval	*P* Value	R^2	Normalized Slope
pfVD						
Foveal VD	−43.679	−0.018	−0.108 to 0.072	0.695	0.953	−0.00088
Average	31.707	−0.051	−0.089 to −0.013	0.008*	0.824	−0.00097
Sup. hemi	31.523	−0.546	−0.951 to −0.148	0.007*	0.768	−0.01034
Inf. hemi	35.717	−0.481	−0.891 to −0.073	0.020*	0.788	−0.00920
T	40.517	−0.068	−0.111 to −0.025	0.002*	0.662	−0.00130
S	29.023	−0.059	−0.107 to −0.012	0.013*	0.816	−0.00111
N	32.069	−0.035	−0.077 to 0.008	0.109	0.712	−0.00066
I	23.904	−0.031	−0.077 to 0.014	0.177	0.673	−0.00059
GCC						
Average	97.558	−0.063	−0.129 to 0.002	0.057	0.971	−0.00065
Sup. hemi	93.999	−0.072	−0.137 to −0.006	0.031*	0.955	−0.00074
Inf. hemi	100.433	−0.061	−0.132 to 0.011	0.094	0.960	−0.00062

* *P* value for an absolute slope different from a zero slope.

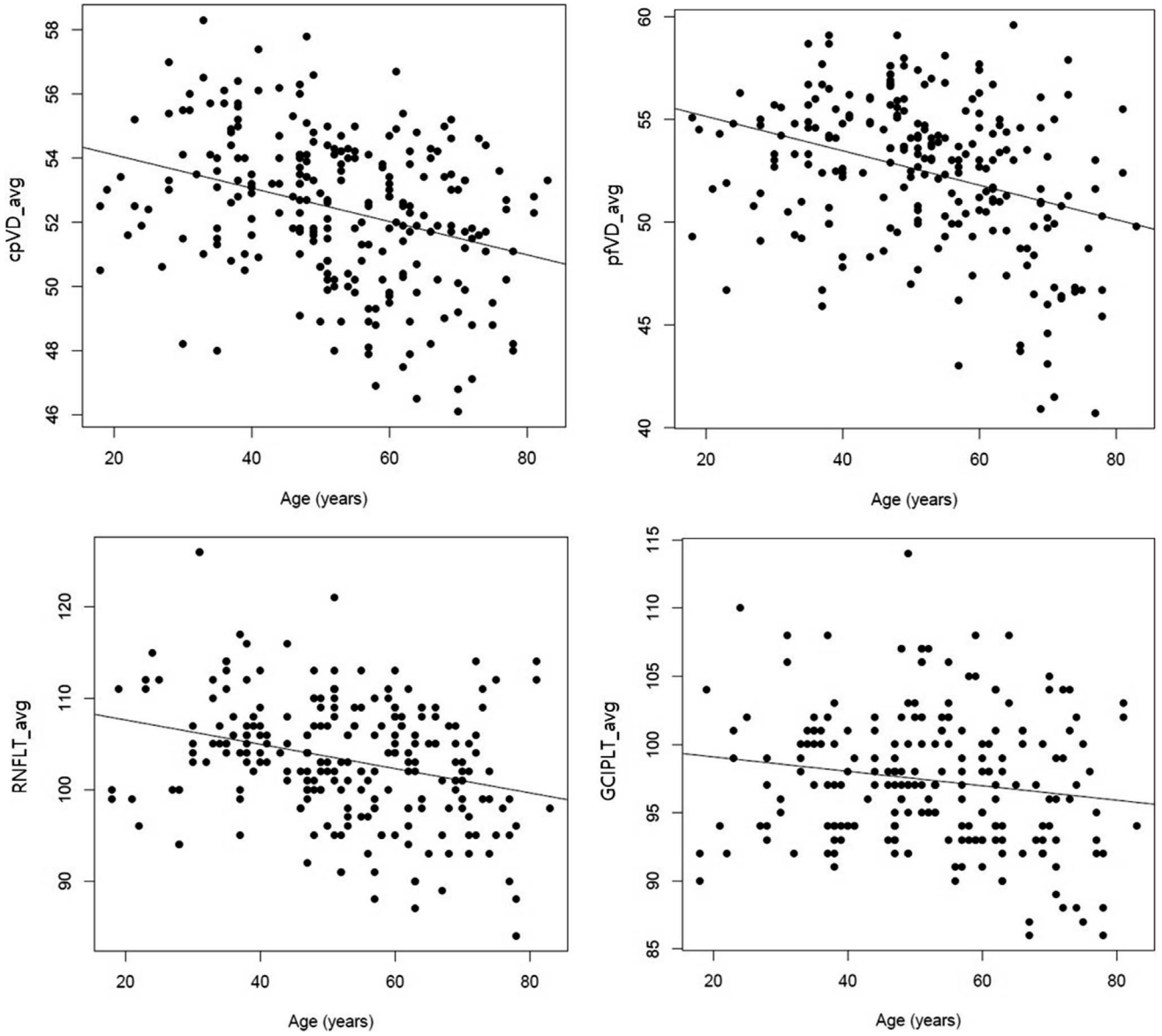

Figure 2. Scatterplots and fitted line for average cpVD, pfVD, RNFL thickness, and GCC thickness.

evaluating true VD changes, but rather looking at the age-related differences in large population. This cross-sectional study can have some artifacts, as can be observed in patients aged 50- to 59-years old, who had lower cpVD than did patients aged 60- to 69-years old (Table 1). Thus, further prospective and longitudinal studies with large number of patients will be needed in the future to elucidate this relationship. Second, OCT-A technology is based on the movement of the blood column to detect the vessels. Therefore, it will not detect the presence of a vessel if there was no movement of the blood column or if the movement was very slow. Third, we did not adjust the scale of the image prior to analysis. However, the parafoveal region has a relatively uniform vascular network in healthy eyes, therefore, small changes from image correction are less likely to induce significant change in overall density.[33] Therefore, we corrected the effect of axial length on VD as a fixed-effect parameter instead of adjusting the scale of the image. Finally, the disc-fovea axis is known as a useful reference to aligning the RNFL sectors over different eyes.[34,35] As the RNFL thickness and cpVD are considered to be related, adjusting cpVD profile to fovea-disc angle axis might explain more of the variance, similarly to RNFL thickness. However, the disc-fovea axis is not available in the current OCT-A software which we used.

In conclusion, we found that most cpVDs decreased with increasing age. The region near the papillomacular bundle showed the shallowest slope among the sectors. Thus, the global and regional changes resulting from the effects of age on VD in the circumpapillary and macular regions should be considered when assessing eyes over time.

Acknowledgments

Disclosure: **Y.H. Jo**, None; **K.R. Sung**, None; **J.W. Shin**, None

References

1. Kashani AH, Chen CL, Gahm JK, et al. Optical coherence tomography angiography: a comprehensive review of current methods and clinical applications. *Prog Retin Eye Res*. 2017; 60:66–100.

2. Jia Y, Wei E, Wang X, et al. Optical coherence tomography angiography of optic disc perfusion in glaucoma. *Ophthalmology*. 2014;121:1322–1332.
3. Yarmohammadi A, Zangwill LM, Diniz-Filho A, et al. Optical coherence tomography angiography vessel density in healthy, glaucoma suspect, and glaucoma eyes. *Invest Ophthalmol Vis Sci*. 2016;57:OCT451–OCT459.
4. Rao HL, Pradhan ZS, Weinreb RN, et al. Regional comparisons of optical coherence tomography angiography vessel density in primary open-angle glaucoma. *Am J Ophthalmol*. 2016; 171:75–83.
5. Lee EJ, Lee KM, Lee SH, Kim T-W. OCT angiography of the peripapillary retina in primary open-angle glaucoma. *Invest Ophthalmol Vis Sci*. 2016;57:6265–6270.
6. Rao HL, Pradhan ZS, Weinreb RN, et al. Determinants of peripapillary and macular vessel densities measured by optical coherence tomography angiography in normal eyes. *J Glaucoma*. 2017;26:491–497.
7. Sacconi R, Borrelli E, Corbelli E, et al. Quantitative changes in the ageing choriocapillaris as measured by swept source optical coherence tomography angiography [published online ahead of print]. *Br J Ophthalmol*. doi:10.1136/bjoph thalmol-2018-313004.
8. Akil H, Huang AS, Francis BA, Sadda SR, Chopra V. Retinal vessel density from optical coherence tomography angiography to differentiate early glaucoma, pre-perimetric glaucoma and normal eyes. *PLoS One*. 2017;12:e0170476.
9. Rao HL, Kadambi SV, Weinreb RN, et al. Diagnostic ability of peripapillary vessel density measurements of optical coherence tomography angiography in primary open-angle and angle-closure glaucoma. *Br J Ophthalmol*. 2017;101:1066–1070.
10. Yu J, Jiang C, Wang X, et al. Macular perfusion in healthy Chinese: an optical coherence tomography angiogram study. *Invest Ophthalmol Vis Sci*. 2015;56:3212–3217.
11. Chalam K, Sambhav K. Optical coherence tomography angiography in retinal diseases. *J Ophthalmic Vis Res*. 2016; 11:84–92.
12. Rao HL, Kadambi SV, Weinreb RN, et al. Diagnostic ability of peripapillary vessel density measurements of optical coherence tomography angiography in primary open-angle and angle-closure glaucoma. *Br J Ophthalmol*. 2017;101:1066–1070.
13. Triolo G, Rabiolo A, Shemonski ND, et al. Optical coherence tomography angiography macular and peripapillary vessel perfusion density in healthy subjects, glaucoma suspects, and glaucoma patients. *Invest Ophthalmol Vis Sci*. 2017;58:5713–5722.
14. Garway-Heath DF, Poinoosawmy D, Fitzke FW, Hitchings RA. Mapping the visual field to the optic disc in normal tension glaucoma eyes. *Ophthalmology*. 2000;107:1809–1815.
15. Rao HL, Pradhan ZS, Weinreb RN, et al. Determinants of peripapillary and macular vessel densities measured by optical coherence tomography angiography in normal eyes. *J Glaucoma*. 2017;26:491–497.
16. Sung MS, Lee TH, Heo H, Park SW. Clinical features of superficial and deep peripapillary microvascular density in healthy myopic eyes. *PLoS One*. 2017;12:e0187160.
17. Holló G. Influence of large intraocular pressure reduction on peripapillary OCT vessel density in ocular hypertensive and glaucoma eyes. *J Glaucoma*. 2017;26:e7–e10.
18. Sung KR, Wollstein G, Bilonick RA, et al. Effects of age on optical coherence tomography measurements of healthy retinal nerve fiber layer, macula, and optic nerve head. *Ophthalmology*. 2009;116:1119–1124.
19. Budenz DL, Anderson DR, Varma R, et al. Determinants of normal retinal nerve fiber layer thickness measured by Stratus OCT. *Ophthalmology*. 2007;114:1046–1052.
20. Alamouti B, Funk J. Retinal thickness decreases with age: an OCT study. *Br J Ophthalmol*. 2003;87:899–901.
21. Parikh RS, Parikh SR, Sekhar GC, Prabakaran S, Babu JG, Thomas R. Normal age-related decay of retinal nerve fiber layer thickness. *Ophthalmology*. 2007;114:921–926.
22. Leung CK-s, Cheung CY-l, Weinreb RN, et al. Retinal nerve fiber layer imaging with spectral-domain optical coherence tomography: a variability and diagnostic performance study. *Ophthalmology*. 2009;116:1257–1263.
23. Patel NB, Lim M, Gajjar A, Evans KB, Harwerth RS. Age-associated changes in the retinal nerve fiber layer and optic nerve head. *Invest Ophthalmol Vis Sci*. 2014;55:5134–5143.
24. Harwerth RS, Wheat JL, Rangaswamy NV. Age-related losses of retinal ganglion cells and axons. *Invest Ophthalmol Vis Sci*. 2008;49:4437–4443.
25. Patel NB, Wheat JL, Rodriguez A, Tran V, Harwerth RS. Agreement between retinal nerve fiber layer measures from Spectralis and Cirrus spectral domain OCT. *Optom Vis Sci*. 2012;89:E652–E666.
26. Celebi ARC, Mirza GE. Age-related change in retinal nerve fiber layer thickness measured with spectral domain optical coherence tomography. *Invest Ophthalmol Vis Sci*. 2013;54: 8095–8103.
27. Feuer WJ, Budenz DL, Anderson DR, et al. Topographic differences in the age-related changes in the retinal nerve fiber layer of normal eyes measured by Stratus™ optical coherence tomography. *J Glaucoma*. 2011;20:133.
28. Lee JY, Hwang YH, Lee SM, Kim YY. Age and retinal nerve fiber layer thickness measured by spectral domain optical coherence tomography. *Korean J Ophthalmol*. 2012;26:163–168.
29. Wang M, Elze T, Li D, et al. Age, ocular magnification, and circumpapillary retinal nerve fiber layer thickness. *J Biomed Opt*. 2017;22:1–19.
30. Mikelberg FS, Drance SM, Schulzer M, Yidegiligne HM, Weis MM. The normal human optic nerve: axon count and axon diameter distribution. *Ophthalmology*. 1989;96:1325–1328.
31. Wang X, Kong X, Jiang C, Li M, Yu J, Sun X. Is the peripapillary retinal perfusion related to myopia in healthy eyes? A prospective comparative study. *BMJ Open*. 2016;6:e010791.
32. Gadde SG, Anegondi N, Bhanushali D, et al. Quantification of vessel density in retinal optical coherence tomography angiography images using local fractal dimension. *Invest Ophthalmol Vis Sci*. 2016;57:246–252.
33. Sampson DM, Gong P, An D, et al. Axial length variation impacts on superficial retinal vessel density and foveal avascular zone area measurements using optical coherence tomography angiography. *Invest Ophthalmol Vis Sci*. 2017; 58:3065–3072.
34. Mwanza JC, Lee G, Budenz DLJAjoo. Effect of adjusting retinal nerve fiber layer profile to fovea-disc angle axis on the thickness and glaucoma diagnostic performance. *Am J Ophthalmol*. 2016;161:12–21.
35. Jonas RA, Wang YX, Yang H, et al. Optic disc-fovea angle: the Beijing Eye Study 2011. *PLoS One*. 2015;10:e0141771.